iScience

CellPress
OPEN ACCESS

Article

Engraftment of adult hematopoietic stem and progenitor cells in a novel model of humanized mice

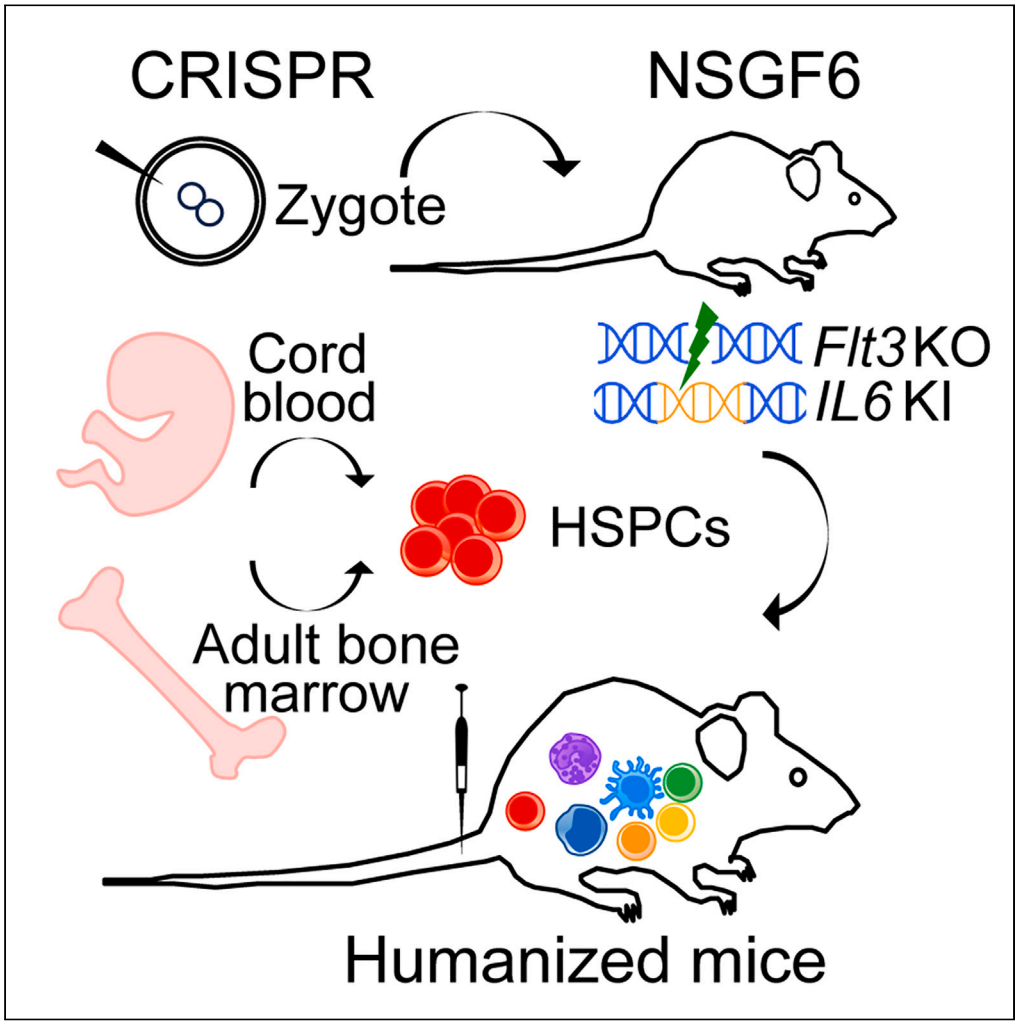

Chun I. Yu, Rick Maser, Florentina Marches, Jacques Banchereau, Karolina Palucka

karolina.palucka@jax.org

Highlights

Humanized mouse model with murine *Flt3* KO and human *IL6* KI

Murine *Flt3* KO and human *IL6* KI support engraftment with fewer HSPCs

Human IL-6 supports human monocyte differentiation

Murine *Flt3* KO and human *IL6* KI support long-term engraftment by adult HSPCs

Yu et al., iScience *27*, 109238
March 15, 2024
https://doi.org/10.1016/j.isci.2024.109238

iScience

CellPress
OPEN ACCESS

Article

Engraftment of adult hematopoietic stem and progenitor cells in a novel model of humanized mice

Chun I. Yu,[1] Rick Maser,[2] Florentina Marches,[1] Jacques Banchereau,[1] and Karolina Palucka[1,3,*]

SUMMARY

Pre-clinical use of humanized mice transplanted with CD34$^+$ hematopoietic stem and progenitor cells (HSPCs) is limited by insufficient engraftment with adult non-mobilized HSPCs. Here, we developed a novel immunodeficient mice based on NOD-SCID-*Il2*$\gamma c^{-/-}$ (NSG) mice to support long-term engraftment with human adult HSPCs. As both Flt3L and IL-6 are critical for many aspects of hematopoiesis, we knock-out mouse *Flt3* and knock-in human *IL6* gene. The resulting mice showed an increase in the availability of mouse Flt3L to human cells and a dose-dependent production of human IL-6 upon activation. Upon transplantation with low number of human HSPCs from adult bone marrow, these humanized mice demonstrated a significantly higher engraftment with multilineage differentiation of human lymphoid and myeloid cells, and tissue colonization at one year after adult HSPC transplant. Thus, these mice enable studies of human hematopoiesis and tissue colonization over time and may facilitate building autologous models for immuno-oncology studies.

INTRODUCTION

Realizing the clinical promise of cancer immunotherapy is hindered by gaps in our knowledge of *in vivo* mechanisms underlying treatment response as well as treatment limiting toxicity. Preclinical *in vivo* model systems are required to address these knowledge gaps and to surmount the challenges faced in the clinical application of immunotherapy. Mice are commonly used for basic and translational research to support development and testing of immune interventions, including for cancer. Yet, despite some remarkable advances, current mouse models share an obvious and important limitation when it comes to translational potential: their immune system is that of a mouse. To overcome this, mice can be humanized through genetic approaches leading to expression of human proteins or through cellular approaches based on transplantation of human cells such as peripheral blood mononuclear cells (PBMCs), fetal bone marrow/liver/thymus tissues (BLT), or human CD34$^+$ hematopoietic stem and progenitor cells (HSPCs).[1–3] However, the allogenic context between human immune cells and cancer cells imposes a confounding factor on the anti-tumor effect. To overcome this, an autologous humanized tumor model is needed, where mice are transplanted with bone marrow-derived HSPCs followed by implantation of patient-derived xenograft (PDX) tumor from the same patient.[4,5]

Humanization by transplanting fetal human CD34$^+$ HSPCs into immunodeficient mice bearing the *Il2rg* mutation has demonstrated human engraftment including T cells[2,3] and has contributed significantly to human immunology research.[6–9] However, model based on NOD-SCID-*Il2*$\gamma c^{-/-}$ (NSG) cannot efficiently support the generation of a diverse and fully functional human immune system for immunology studies. Various efforts have been made to genetically engineer human cytokines to cross mouse and human barriers.[10] Human growth factors including granulocyte-colony stimulating factor (G-CSF), granulocyte macrophage colony stimulating factor (GM-CSF), macrophage colony stimulating factor (M-CSF), interleukin (IL)-3, IL-6, IL-15, IL-34, and stem cell factor (SCF) have been shown to impact human hematopoiesis which led to adequate development of human hematopoietic lineages in humanized mice.[7,11–19] Nevertheless, few humanized mouse models have reported engraftment by human adult bone marrow-derived HSPC and myeloid cell development.[5,20,21]

FMS-like tyrosine kinase 3 Ligand (Flt3L) and IL-6 are cytokines important for hematopoiesis. Loss-of-function mutation in murine *Flt3* (FMS-like tyrosine kinase 3) leads to a decrease in mouse dendritic cells (DCs) and an accumulation of mouse ligand in the serum.[22–24] This could lead to the creation of "space" in peripheral tissues enabling colonization with human cells upon HSPC transplant as well as increased availability of murine Flt3L to the human receptor, supporting development of human immune cells including DCs[25] and B cells.[26] IL-6 lacks cross-reactivity between mouse and human, and it plays key roles in the innate and adaptive immune systems, including HSPC survival,[27] monocyte differentiation to macrophages by facilitation of autocrine CSF-1 internalization,[28] and the differentiation of follicular helper

[1]The Jackson Laboratory for Genomic Medicine (JAX-GM), Farmington, CT 06032, USA
[2]The Jackson Laboratory for Mammalian Genetics (JAX-MG), Bar Harbor, ME 04609, USA
[3]Lead contact
*Correspondence: karolina.palucka@jax.org
https://doi.org/10.1016/j.isci.2024.109238

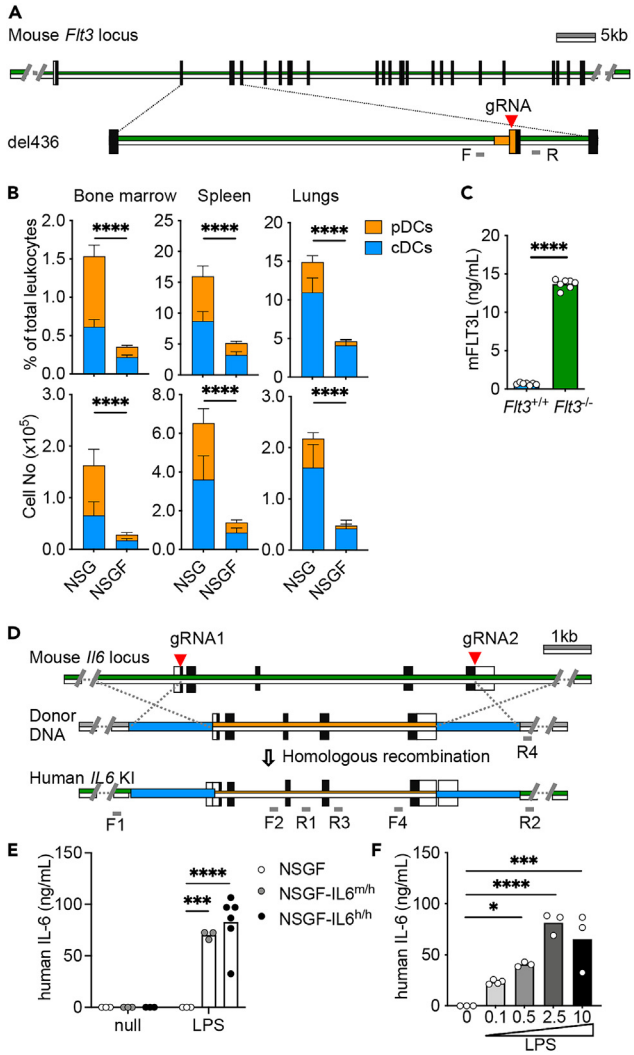

Figure 1. Genetic engineering of novel NSG mice via CRISPR

(A) Schematic representation of CRISPR/Cas9 at mouse *Flt3* locus and the chromosomal deletion at the exon 3. Green lines represent the mouse sequences and orange lines represent the mutated sequences. Black boxes represent the coding region and white box represent the non-coding region. gRNAs are labeled with red arrowhead and the primer pairs F/R are in gray.

(B) The summary of percentage (upper) and total number (lower) of mouse pDCs and cDCs from bone marrow, spleen and lungs of 8–10 weeks of mice (mean ± SD, n = 7).

(C) Mouse Flt3L in the plasma of 8–10 weeks old mice were analyzed by ELISA (mean, n = 7).

(D) Schematic representation of CRISPR/Cas9 at mouse *Il6* locus, the vector for human *IL6* donor DNA and targeted allele with homologous recombination. Green lines represent the mouse sequences and orange lines represent the human *IL6* sequences. Black boxes represent the coding region and white box represent the non-coding region. gRNAs are labeled with red arrowhead. Blue boxes represent the left and right homologous arms. One of the primer pairs F1/R1 and F2/R2 in gray is located outside of the homologous arms, respectively.

(E) Human IL-6 production (mean, n = 3–6) in the plasma of mice collected at 2 h after i.p. treatment of LPS (10 μg).

(F) Human IL-6 production (mean, n = 3) in the plasma of mice collected at 2 h after i.p. treatment of LPS (0.1, 0.5, 2.5, or 10 μg).

See also Figure S1.

T cells, and antibody producing plasma cells.[29–32] Thus, we knocked out (KO) mouse *Flt3* in order to increase the availability of mouse Flt3L (which can act via human receptor) to human cells, thereby improving the long-term development of human myeloid cells upon transplantation with human CD34$^+$ HSPCs.[33] We then genetically engineered the mice to express human IL-6. This novel mouse model yielded a higher human engraftment and supported long-term multilineage development of human immune cells when transplanted with adult human CD34$^+$ HSPCs.

RESULTS

Construction of murine *Flt3* KO and human *IL6* KI mice via CRISPR

We first used the clustered regularly interspaced short palindromic repeats (CRISPR)/CRISPR-associated protein-9 nuclease (Cas9) system to generate NSG mice with *Flt3* KO (NSGF).[34] Founder mice carrying a chromosomal deletion at the exon 3 were backcrossed to NSG mice and inbred to obtain homozygous *Flt3*$^{-/-}$ allele confirmed by PCR and Sanger sequence (Figures 1A and S1A). NSGF mice were healthy and indistinguishable from NSG mice in appearance. To verify the impact of *Flt3* KO, we analyzed different mouse myeloid cells and subsets of DCs including CD317^{+} plasmacytoid DCs (pDCs), CD11c^{+} conventional DCs (cDCs) by flow cytometry (Figure S1B). As expected, we observed an 80% decrease in both pDCs and cDC in the bone marrow, spleen, and lungs of NSGF mice in comparison to age and gender matched NSG mice (Figures 1B and S1C). We observed an overall slight decrease in other myeloid cells (Figure S1D). As expected, we found an increased amount of mouse Flt3L in the plasma of NSGF mice (Figure 1C).

Next, we generated human *IL6* knockin (KI) to replace mouse ortholog using CRISPR/Cas9 gene targeting in zygotes and inserting the full-length of human *IL6* gene sequence into exon 1 and exon 5 of mouse *Il6* locus via homologous recombination (Figure 1D). Founder mice were selected first with PCR assays targeting 5′ and 3′ junctions and full-length sequence between two homology arms. We confirmed the absence of plasmid donor sequences to discern correct on-target single copy integration events from random or multi-copy targeting events. Sequencing of these PCR products confirmed proper targeting of human *IL6*. Five founder mice with on-target single copy integration events of human *IL6* KI were identified (Figure S1D). Founder mice with human *IL6* KI were first bred to NSGF mice and then intercrossed to generate homozygous animals for *IL6* targeted mutation (NSGF6). Human IL-6 was found in the plasma of mice with *IL6*$^{m/h}$ and *IL6*$^{h/h}$ genotypes but not wild-type mice upon i.p. challenge with LPS in a dose-dependent manner (Figures 1E and 1F).

Human *IL6* KI boosts HSPC engraftment and human monocyte differentiation

As IL-6 promotes HSPC survival,[27] we first analyzed engraftment with cord blood CD34^{+} HSPCs to test whether human *IL6* KI improves humanization. To this end, sublethally irradiated NSG and NSGF6 mice at 4-week of age were first transplanted with titrated amount of cord blood CD34^{+} HSPCs. Female mice were used here due to higher engraftment rates as compared to male mice.[35,36] Comparable engraftment was found in the blood of mice transplanted with high number of HSPCs (1x10^{5}) from cord blood (Figure 2A). Yet humanized (h)NSGF6 mice but not hNSG mice were consistently engrafted when transplanted with low number of cord blood HSPCs (1x10^{4}) (Figures 2A and S2). This difference in engraftment was found in the blood up to six-month follow-up (Figure 2B). Furthermore, improvement was found in both CD33^{+} myeloid cell and CD3^{+} T cell development with a significant increase in the absolute cell counts (Figure 2C). We also observed the presence of different monocyte subsets with a significant increase in CD16^{+} non-classical monocytes in the blood (Figure 2D). Predominately CD45RA^{+} CCR7^{+} naive T cells were found in the blood at 16-week after HSPC transplant (Figure 2E). Thus, we conclude that mouse *Flt3* KO and human *IL6* KI improve the engraftment of human immune cells both quantitatively and qualitatively upon transplant with human cord blood CD34^{+} HSPCs.

To determine whether human *IL6* KI is essential for monocyte subset differentiation, we compared NSGF6 mice with NSGF mice using high number of cord blood HSPCs (1x10^{5}). As expected, similar engraftment with different lineages of human immune cells was found in various tissues of hNSGF and hNSGF6 mice with slight variability found among mice (Figures 3A, S3, and S4). However, in comparison to hNSGF mice, significantly higher frequencies of CD14^{+} cells were found in the spleen and lungs of hNSGF6 mice (Figure 3B). We also found higher frequencies of both CD14^{+}CD16^{+} and CD14^{low}CD16^{+} monocytes in the spleen and lungs of hNSGF6 mice engrafted with cord blood HSPCs (Figures 3C and 3D). Thus, our data corroborate other studies[16] and demonstrate that human IL-6 is important for the development of CD16^{+} monocytes.

Murine *Flt3* KO and human *IL6* KI support long-term engraftment by adult HSPCs

The key question was if our novel model enables engraftment of adult bone marrow HSPCs which thus far has proven difficult in other models. To this end, we transplanted 1 × 10^{5} bone marrow-derived CD34^{+} HSPCs into sublethally irradiated NSG and NSGF6 mice. As shown in Figure 4, we found significantly higher hCD45^{+} engraftment in the blood of hNSGF6 mice than in hNSG mice (Figures 4A and S2). Human CD33^{+} myeloid cells, CD19^{+} B cells, and CD3^{+} T cells were all present in significantly higher numbers in the blood of hNSGF6 mice than hNSG mice (Figure 4B). Consistent with cord blood HSPCs, we also observed a significant increase in CD14^{+} monocytes (Figure 4C), and predominately CD45RA^{+} CCR7^{+} naive T cells in the blood at 16-week after bone marrow HSPC transplant (Figure 4D). Furthermore, hNSGF6 mice demonstrated superior overall engraftment than hNSG mice over one-year follow-up (Figure 5A). hCD33^{+} myeloid cells were consistently present in the blood of hNSGF6 mice (Figure 5B). In contrast to the persistent lack of T cell developments in hNSG mice, circulating CD3^{+} T cells were found in hNSGF6 mice as early as 16 weeks, reached plateau at 24 weeks and remained persistent up to one year follow-up (Figures 5B and 5C). Additionally, we found a stable presence of CD45RA^{+}CCR7^{+} naive T cells in addition to an expansion or accumulation of CD4^{+} T cells with memory phenotype (Figure 5D). Finally, we analyzed the human immune composition in the tissues of humanized mice at one year after engraftment with bone marrow HSPCs. In comparison to hNSG mice, hNSGF6 mice showed significantly higher percentage of CD11c^{+} cDCs and CD56^{+} NK cells in bone marrow; and substantial increase in many lineages of human immune cells including CD15^{+} or CD66b^{+} granulocytes, CD14^{+} monocytes, CD11c^{+} cDCs, CD19^{+} B cells, CD56^{+} NK cells, and CD4^{+} T cells in the spleen or lungs (Figures 5E and S3). Consistently, we also found a significantly higher frequency of total CD14^{+} monocytes with CD14^{+}CD16^{+} and CD14^{low}CD16^{+} phenotype in the spleen and lungs of hNSGF6 mice (Figure 5F). Thus, human *IL6* KI combined with *Flt3* KO improves the engraftment and long-term development of human immune cells upon transplant with human adult non-mobilized CD34^{+} HSPCs.

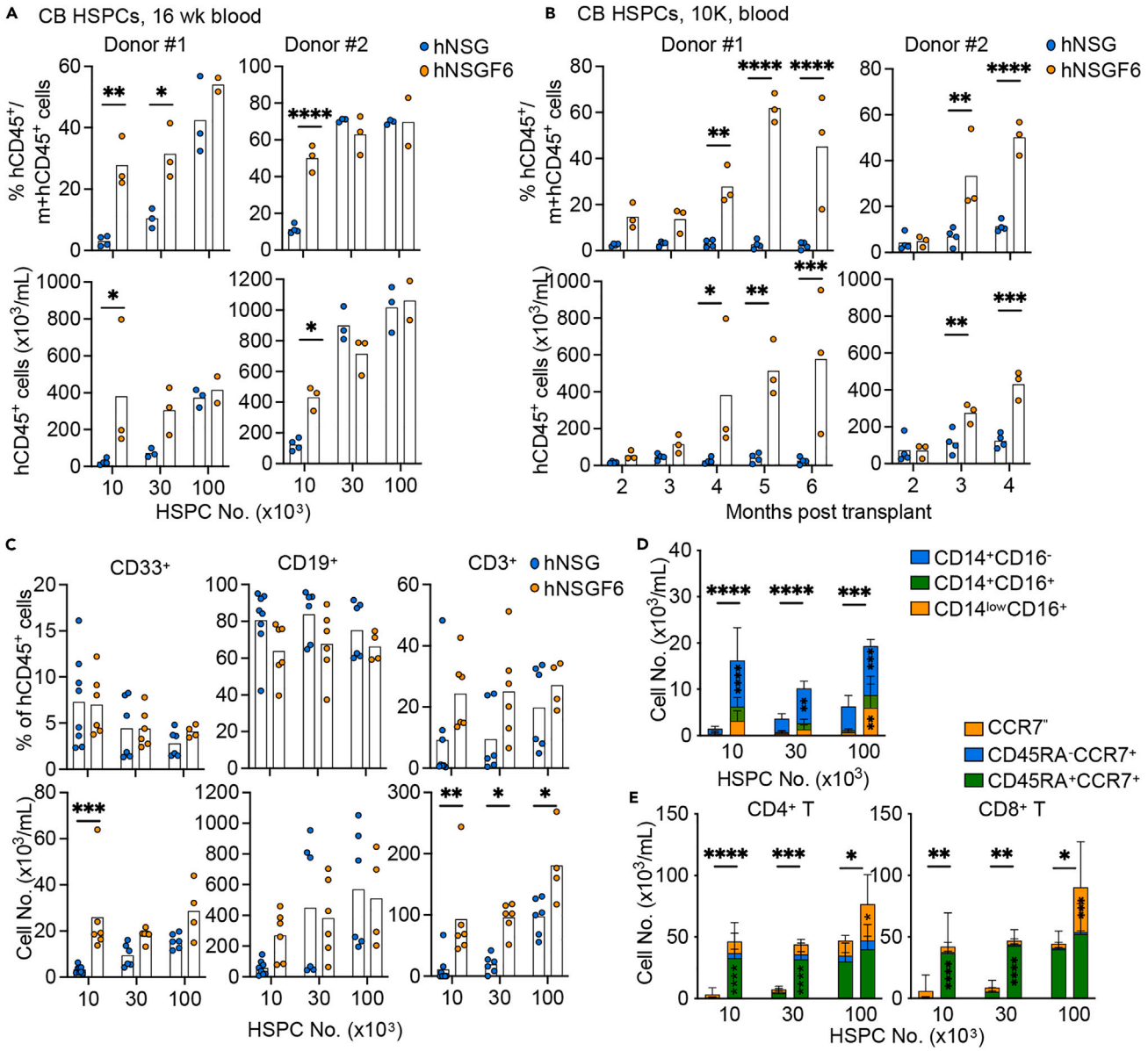

Figure 2. Improved human engraftment by HSPCs from cord blood

(A) NSG or NSGF6 mice were transplanted with 1x10^4, 3x10^4, and 1x10^5 HSPCs from cord blood at 4-week of age. Human engraftment in the blood by the mean percentage (upper) and absolute number (lower) of hCD45$^+$ cells at 16 weeks after transplant. n = 2–4 mice from two independent experiments. two-way ANOVA.

(B) The kinetics of mean human engraftment in the blood in hNSG or hNSGF6 mice after transplant of 1x10^4 cord blood HSPCs. n = 3–4 mice from two independent experiments. two-way ANOVA.

(C) The mean percentage (upper) and absolute number (lower) of human CD33$^+$ myeloid cells, CD19$^+$ B cells, and CD3$^+$ T cells in the blood at 16 weeks after transplant. n = 4–8 mice pooled from two donors. two-way ANOVA.

(D) The absolute number of human CD14$^+$ monocyte subsets in the blood at 16 weeks after transplant (mean ± SD, n = 4–8). two-way ANOVA.

(E) The absolute number of human CD4$^+$ CD3$^+$ (left) or CD8$^+$ CD3$^+$ T cell subsets in the blood at 16 weeks after transplant (mean ± SD, n = 4–8). two-way ANOVA.

See also Figure S2.

DISCUSSION

In summary, we have developed a novel strain of immunodeficient mice which enables robust multilineage development of human immune cells in tissues when engrafted with CD34$^+$ HSPCs from adult bone marrow. The higher engraftment in the peripheral of hNSGF6 mice is likely due to the combined effects of both murine *Flt3* KO and human *IL6* KI. *Flt3* KO eliminates both murine DC and other myeloid cell development which opens up the niches and enables the repopulation of human DC, other myeloid cells, B cells and T cells due to the increased

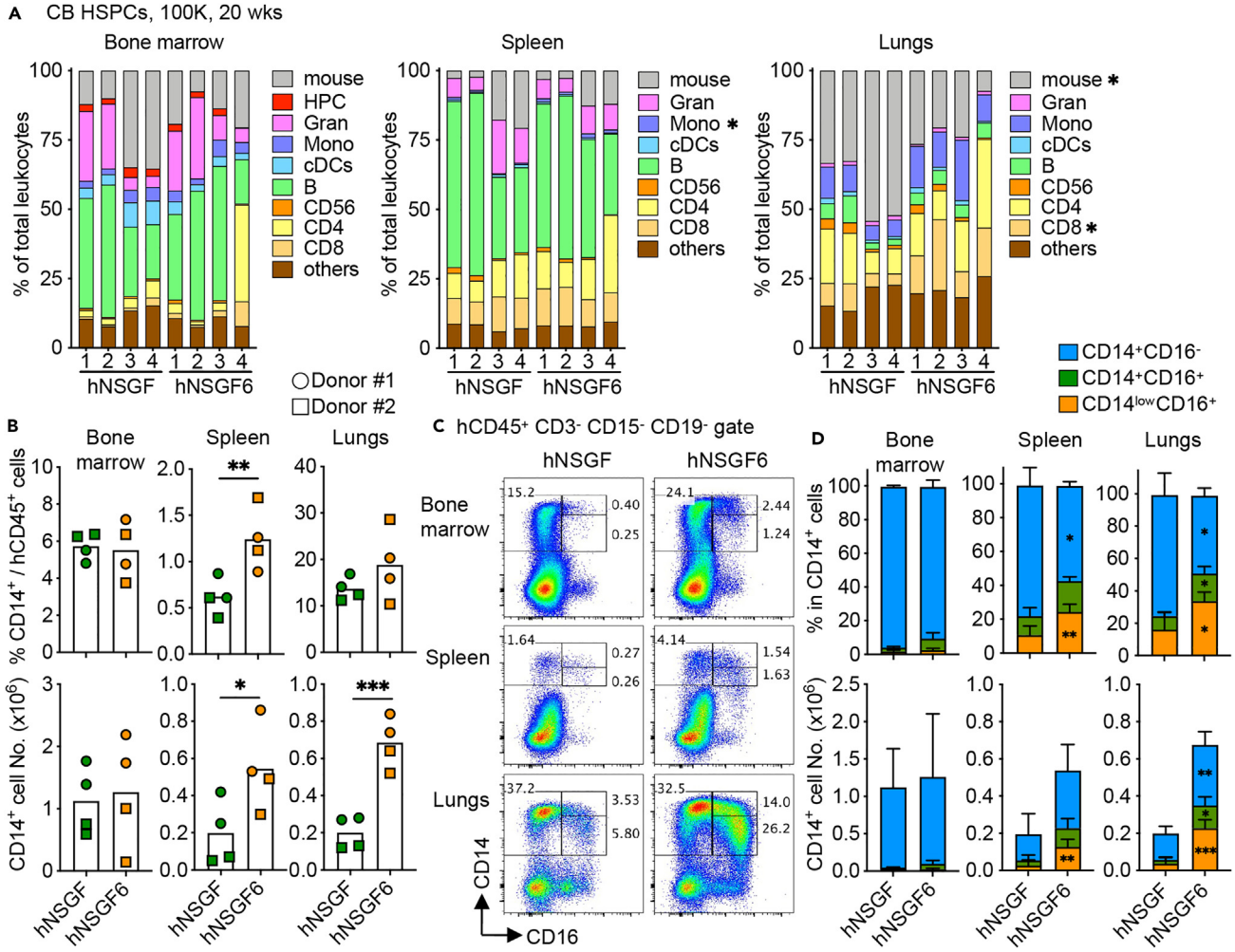

Figure 3. Human IL-6 supports human monocyte differentiation

(A) The percentage of human immune cell type in total CD45$^+$ leukocytes (mouse and human) in the bone marrow, spleen, and lungs of hNSGF and hNSGF6 at 20-week post-transplant with cord blood HSPCs. n = 4 from two donors. two-tailed t test.

(B) Summary of the mean percentage (upper panels) and absolute number (lower panels) of CD14$^+$ cells in mice. n = 4 from two donors. two-tailed t test.

(C) Representative FACS plots of human monocyte subsets.

(D) Summary of CD14$^+$ cell subsets (mean ± SD, n = 4). two-way ANOVA.

Gran, granulocytes; Mono, monocytes.

See also Figures S3 and S4.

availability of cross-reactive mouse Flt3L and human IL-6.[17,33] Indeed, IL-6 has been shown to expand memory and/or effector T cells by limiting apoptosis and promoting T cells survival. IL-6 mediated STAT3-dependent upregulation of anti-apoptotic regulator in Bcl-2 and Bcl-xL and downregulation of Fas surface expression.[37–40] Hence, our new model should improve generation of autologous models and enhance our ability to investigate human tumor-human immune system interactions in humanized mice.

Limitations of study

Although the number of humanized mice was small due to the limitation on the number of the CD34$^+$ HSPCs available from cord blood or adult bone marrow, the data consistently demonstrated that NSGF6 mice support higher engraftment with fewer CD34$^+$ HSPCs. Furthermore, female mice were used here for their capacity to better support human HSPC engraftment. Future work should aim to further dissect the functionality of the developed cell types, and how this new mouse model could benefit autologous models for immuno-oncology studies.

STAR★METHODS

Detailed methods are provided in the online version of this paper and include the following:

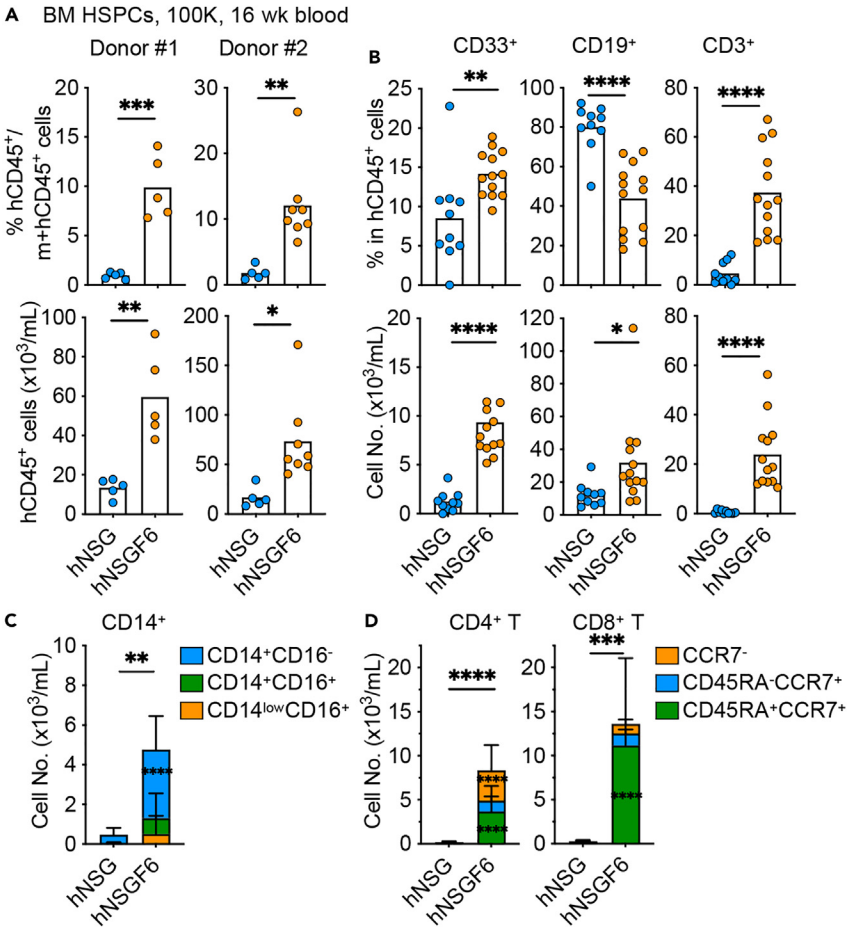

Figure 4. Improved human engraftment by adult HSPCs

(A) Humanized mice were generated by engrafting NSG and NSGF6 mice with 1x10^5 bone marrow HSPCs. The mean percentage (upper) and absolute number (lower) of hCD45$^+$ cells at 16 weeks after transplant. n = 5–8 mice from two donors. two-tailed t test.

(B) The mean percentage (upper) and absolute number (lower) of human CD33$^+$ myeloid cells, CD19$^+$ B cells and CD3$^+$ T cells in the blood at 16 weeks after transplant. n = 10–13 mice pooled from two donors. two-tailed t test.

(C) The absolute number of human CD14$^+$ monocyte subsets in the blood at 16 weeks after transplant (mean ± SD, n = 10–13). two-way ANOVA.

(D) The absolute number of human CD4$^+$ CD3$^+$ (left) or CD8$^+$CD3$^+$T cell subsets in the blood at 16 weeks after transplant (mean ± SD, n = 10–13). two-way ANOVA.

See also Figure S2.

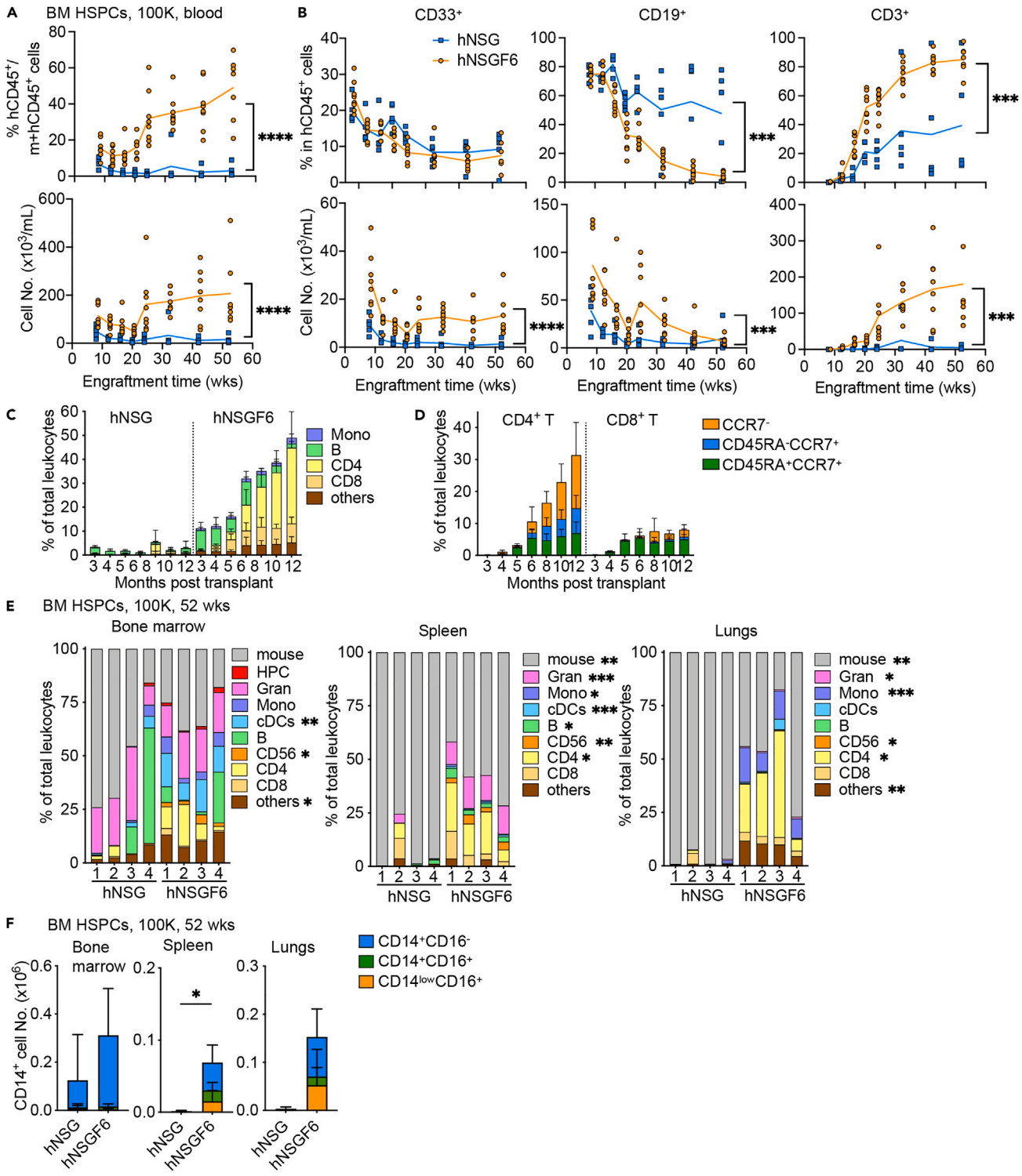

Figure 5. Murine *Flt3* KO and human *IL6* KI support long-term engraftment by adult HSPCs

(A) The kinetics of mean percentage (upper panel) and absolute number (lower panel) of hCD45$^+$ cells in the blood of NSG and NSGF6 mice at different time points after transplant with 1x10^5 bone marrow HSPCs. n = 5–8 from one donor. two-way ANOVA.

(B) The kinetics of mean percentage (upper panel) and absolute number (lower panel) of human CD33$^+$ myeloid cells, CD3$^+$ T cells, and CD19$^+$ B cells (mean, n = 5–8 mice) in the blood. one-way ANOVA.

Figure 5. *Continued*

(C) The percentage of different human immune cell types in total CD45$^+$ leukocytes (mouse and human) analyzed at different time points after HSPC transplant in the blood (mean ± SD, n = 5–8 mice).

(D) Kinetics of human CCR7$^+$ CD45RA$^+$ naive, CCR7$^+$ CD45RA$^-$ central memory, and CCR7$^-$ effector CD4$^+$ or CD8$^+$ T cell frequency in the blood of hNSGF6 mice (mean ± SD, n = 5–8 mice).

(E) The percentage of different human immune cell types in total CD45$^+$ leukocytes (mouse and human) in the bone marrow, spleen and lungs analyzed at one year post transplant by FACS. n = 4 mice from one bone marrow donor. two-tailed t test.

(F) Summary of the CD14$^+$ cell subsets (mean ± SD, n = 4 mice). two-tailed t test.

See also Figure S3.

SUPPLEMENTAL INFORMATION

Supplemental information can be found online at https://doi.org/10.1016/j.isci.2024.109238.

ACKNOWLEDGMENTS

We thank healthy donors for participation in our studies over the years. We thank Dr. Lenny Shultz for discussion; Pierre Authie, Patrick Metang, Vanessa KP Oliveria, Mayerlin Chalarca, Michael Michaud and PDX core at JAX-MG for help with mice; GET at JAX-MG for help with mouse model generation; Transgenic Genotyping Service at JAX-MG; Breeding Service and Research Animal Facility at JAX-MG; Molecular Diagnostics at JAX-MG; Comparative Medicine and Quality Service at JAX-MG; Comparative Medicine at UCHC. This work was supported by grants from The Jackson Laboratory Director Innovation Fund and NIH (P30 CA034196, R01 CA219880, and R21 OD032454).

AUTHOR CONTRIBUTIONS

Conceptualization, C.Y., J.B., and K.P.; methodology, C.Y., R.M, and F.M.; investigation, C.Y., R.M., and F.M.; writing – original draft, C.Y., R.M., F.M., J.B., and K.P.; writing – review & editing, C.Y. and K.P.

DECLARATION OF INTERESTS

C.Y., R.M., J.B., and K.P filed a patent on novel humanized mouse models via genetic editing of NSG mouse. K.P. is a stockholder in Cue Biopharma and Guardian Bio, scientific advisor to Cue Biopharma and Guardian Bio and co-founder of Guardian Bio. K.P. declares unrelated funding support from Guardian Bio (current) and MERCK (past). J.B. is associated with Immunai.

Received: October 4, 2023
Revised: January 29, 2024
Accepted: February 9, 2024
Published: February 15, 2024

REFERENCES

1. Garcia, J.V. (2016). In vivo platforms for analysis of HIV persistence and eradication. J. Clin. Invest. *126*, 424–431. https://doi.org/10.1172/JCI80562.
2. Traggiai, E., Chicha, L., Mazzucchelli, L., Bronz, L., Piffaretti, J.C., Lanzavecchia, A., and Manz, M.G. (2004). Development of a human adaptive immune system in cord blood cell-transplanted mice. Science *304*, 104–107. https://doi.org/10.1126/science.1093933.
3. Matsumura, T., Kametani, Y., Ando, K., Hirano, Y., Katano, I., Ito, R., Shiina, M., Tsukamoto, H., Saito, Y., Tokuda, Y., et al. (2003). Functional CD5+ B cells develop predominantly in the spleen of NOD/SCID/gammac(null) (NOG) mice transplanted either with human umbilical cord blood, bone marrow, or mobilized peripheral blood CD34+ cells. Exp. Hematol. *31*, 789–797.
4. Fu, J., Sen, R., Masica, D.L., Karchin, R., Pardoll, D., Walter, V., Hayes, D.N., Chung, C.H., and Kim, Y.J. (2017). Autologous reconstitution of human cancer and immune system in vivo. Oncotarget *8*, 2053–2068. https://doi.org/10.18632/oncotarget.14026.
5. Chiorazzi, M., Martinek, J., Krasnick, B., Zheng, Y., Robbins, K.J., Qu, R., Kaufmann, G., Skidmore, Z., Juric, M., Henze, L.A., et al. (2023). Autologous humanized PDX modeling for immuno-oncology recapitulates features of the human tumor microenvironment. J. Immunother. Cancer *11*, e006921. https://doi.org/10.1136/jitc-2023-006921.
6. Saito, Y., Shultz, L.D., and Ishikawa, F. (2020). Understanding Normal and Malignant Human Hematopoiesis Using Next-Generation Humanized Mice. Trends Immunol. *41*, 706–720. https://doi.org/10.1016/j.it.2020.06.004.
7. Theocharides, A.P.A., Rongvaux, A., Fritsch, K., Flavell, R.A., and Manz, M.G. (2016). Humanized hemato-lymphoid system mice. Haematologica *101*, 5–19. https://doi.org/10.3324/haematol.2014.115212.
8. Legrand, N., Ploss, A., Balling, R., Becker, P.D., Borsotti, C., Brezillon, N., Debarry, J., de Jong, Y., Deng, H., Di Santo, J.P., et al. (2009). Humanized mice for modeling human infectious disease: challenges, progress, and outlook. Cell Host Microbe *6*, 5–9. https://doi.org/10.1016/j.chom.2009.06.006.
9. Ito, R., Takahashi, T., and Ito, M. (2018). Humanized mouse models: Application to human diseases. J. Cell. Physiol. *233*, 3723–3728. https://doi.org/10.1002/jcp.26045.
10. Willinger, T., Rongvaux, A., Strowig, T., Manz, M.G., and Flavell, R.A. (2011). Improving human hemato-lymphoid-system mice by cytokine knock-in gene replacement. Trends Immunol. *32*, 321–327. https://doi.org/10.1016/j.it.2011.04.005.
11. Jangalwe, S., Shultz, L.D., Mathew, A., and Brehm, M.A. (2016). Improved B cell development in humanized NOD-scid IL2Rgamma(null) mice transgenically expressing human stem cell factor, granulocyte-macrophage colony-stimulating factor and interleukin-3. Immun. Inflamm. Dis. *4*, 427–440. https://doi.org/10.1002/iid3.124.
12. Cosgun, K.N., Rahmig, S., Mende, N., Reinke, S., Hauber, I., Schäfer, C., Petzold, A., Weisbach, H., Heidkamp, G., Purbojo, A., et al. (2014). Kit regulates HSC engraftment across the human-mouse species barrier. Cell Stem Cell *15*, 227–238. https://doi.org/10.1016/j.stem.2014.06.001.
13. Willinger, T., Rongvaux, A., Takizawa, H., Yancopoulos, G.D., Valenzuela, D.M., Murphy, A.J., Auerbach, W., Eynon, E.E., Stevens, S., Manz, M.G., and Flavell, R.A. (2011). Human IL-3/GM-CSF knock-in mice

support human alveolar macrophage development and human immune responses in the lung. Proc. Natl. Acad. Sci. USA *108*, 2390–2395. https://doi.org/10.1073/pnas.1019682108.

14. Rathinam, C., Poueymirou, W.T., Rojas, J., Murphy, A.J., Valenzuela, D.M., Yancopoulos, G.D., Rongvaux, A., Eynon, E.E., Manz, M.G., and Flavell, R.A. (2011). Efficient differentiation and function of human macrophages in humanized CSF-1 mice. Blood *118*, 3119–3128. https://doi.org/10.1182/blood-2010-12-326926.
15. Huntington, N.D., Alves, N.L., Legrand, N., Lim, A., Strick-Marchand, H., Mention, J.J., Plet, A., Weijer, K., Jacques, Y., Becker, P.D., et al. (2011). IL-15 transpresentation promotes both human T-cell reconstitution and T-cell-dependent antibody responses in vivo. Proc. Natl. Acad. Sci. USA *108*, 6217–6222. https://doi.org/10.1073/pnas.1019167108.
16. Hanazawa, A., Ito, R., Katano, I., Kawai, K., Goto, M., Suemizu, H., Kawakami, Y., Ito, M., and Takahashi, T. (2018). Generation of Human Immunosuppressive Myeloid Cell Populations in Human Interleukin-6 Transgenic NOG Mice. Front. Immunol. *9*, 152. https://doi.org/10.3389/fimmu.2018.00152.
17. Yu, H., Borsotti, C., Schickel, J.N., Zhu, S., Strowig, T., Eynon, E.E., Frleta, D., Gurer, C., Murphy, A.J., Yancopoulos, G.D., et al. (2017). A novel humanized mouse model with significant improvement of class-switched, antigen-specific antibody production. Blood *129*, 959–969. https://doi.org/10.1182/blood-2016-04-709584.
18. Mathews, S., Branch Woods, A., Katano, I., Makarov, E., Thomas, M.B., Gendelman, H.E., Poluektova, L.Y., Ito, M., and Gorantla, S. (2019). Human Interleukin-34 facilitates microglia-like cell differentiation and persistent HIV-1 infection in humanized mice. Mol. Neurodegener. *14*, 12. https://doi.org/10.1186/s13024-019-0311-y.
19. Rongvaux, A., Willinger, T., Martinek, J., Strowig, T., Gearty, S.V., Teichmann, L.L., Saito, Y., Marches, F., Halene, S., Palucka, A.K., et al. (2014). Development and function of human innate immune cells in a humanized mouse model. Nat. Biotechnol. *32*, 364–372. https://doi.org/10.1038/nbt.2858.
20. Saito, Y., Ellegast, J.M., Rafiei, A., Song, Y., Kull, D., Heikenwalder, M., Rongvaux, A., Halene, S., Flavell, R.A., and Manz, M.G. (2016). Peripheral blood CD34(+) cells efficiently engraft human cytokine knock-in mice. Blood *128*, 1829–1833. https://doi.org/10.1182/blood-2015-10-676452.
21. Beyer, A.I., and Muench, M.O. (2017). Comparison of Human Hematopoietic Reconstitution in Different Strains of Immunodeficient Mice. Stem Cells Dev. *26*, 102–112. https://doi.org/10.1089/scd.2016.0083.
22. Sitnicka, E., Bryder, D., Theilgaard-Mönch, K., Buza-Vidas, N., Adolfsson, J., and Jacobsen, S.E.W. (2002). Key Role of flt3 Ligand in Regulation of the Common Lymphoid Progenitor but Not in Maintenance of the Hematopoietic Stem Cell Pool. Immunity *17*, 463–472.
23. Karsunky, H., Merad, M., Cozzio, A., Weissman, I.L., and Manz, M.G. (2003). Flt3 ligand regulates dendritic cell development from Flt3+ lymphoid and myeloid-committed progenitors to Flt3+ dendritic cells in vivo. J. Exp. Med. *198*, 305–313.
24. McKenna, H.J., Stocking, K.L., Miller, R.E., Brasel, K., De Smedt, T., Maraskovsky, E., Maliszewski, C.R., Lynch, D.H., Smith, J., Pulendran, B., et al. (2000). Mice lacking flt3 ligand have deficient hematopoiesis affecting hematopoietic progenitor cells, dendritic cells, and natural killer cells. Blood *95*, 3489–3497.
25. Maraskovsky, E., Daro, E., Roux, E., Teepe, M., Maliszewski, C.R., Hoek, J., Caron, D., Lebsack, M.E., and McKenna, H.J. (2000). In vivo generation of human dendritic cell subsets by Flt3 ligand. Blood *96*, 878–884.
26. Miller, J.S., McCullar, V., Punzel, M., Lemischka, I.R., and Moore, K.A. (1999). Single adult human CD34(+)/Lin-/CD38(-) progenitors give rise to natural killer cells, B-lineage cells, dendritic cells, and myeloid cells. Blood *93*, 96–106.
27. Moldenhauer, A., Genter, G., Lun, A., Bal, G., Kiesewetter, H., and Salama, A. (2008). Hematopoietic progenitor cells and interleukin-stimulated endothelium: expansion and differentiation of myeloid precursors. BMC Immunol. *9*, 56. https://doi.org/10.1186/1471-2172-9-56.
28. Chomarat, P., Banchereau, J., Davoust, J., and Palucka, A.K. (2000). IL-6 switches the differentiation of monocytes from dendritic cells to macrophages. Nat. Immunol. *1*, 510–514. https://doi.org/10.1038/82763.
29. Jego, G., Palucka, A.K., Blanck, J.P., Chalouni, C., Pascual, V., and Banchereau, J. (2003). Plasmacytoid dendritic cells induce plasma cell differentiation through type I interferon and interleukin 6. Immunity *19*, 225–234.
30. Nurieva, R.I., Chung, Y., Martinez, G.J., Yang, X.O., Tanaka, S., Matskevitch, T.D., Wang, Y.H., and Dong, C. (2009). Bcl6 mediates the development of T follicular helper cells. Science *325*, 1001–1005. https://doi.org/10.1126/science.1176676.
31. Papillion, A., Powell, M.D., Chisolm, D.A., Bachus, H., Fuller, M.J., Weinmann, A.S., Villarino, A., O'Shea, J.J., León, B., Oestreich, K.J., and Ballesteros-Tato, A. (2019). Inhibition of IL-2 responsiveness by IL-6 is required for the generation of GC-TFH cells. Sci. Immunol. *4*, eaaw7636. https://doi.org/10.1126/sciimmunol.aaw7636.
32. Das, R., Strowig, T., Verma, R., Koduru, S., Hafemann, A., Hopf, S., Kocoglu, M.H., Borsotti, C., Zhang, L., Branagan, A., et al. (2016). Microenvironment-dependent growth of preneoplastic and malignant plasma cells in humanized mice. Nat. Med. *22*, 1351–1357. https://doi.org/10.1038/nm.4202.
33. Li, Y., Mention, J.J., Court, N., Masse-Ranson, G., Toubert, A., Spits, H., Legrand, N., Corcuff, E., Strick-Marchand, H., and Di Santo, J.P. (2016). A novel Flt3-deficient HIS mouse model with selective enhancement of human DC development. Eur. J. Immunol. *46*, 1291–1299. https://doi.org/10.1002/eji.201546132.
34. Wang, H., Yang, H., Shivalila, C.S., Dawlaty, M.M., Cheng, A.W., Zhang, F., and Jaenisch, R. (2013). One-step generation of mice carrying mutations in multiple genes by CRISPR/Cas-mediated genome engineering. Cell *153*, 910–918. https://doi.org/10.1016/j.cell.2013.04.025.
35. Notta, F., Doulatov, S., and Dick, J.E. (2010). Engraftment of human hematopoietic stem cells is more efficient in female NOD/SCID/IL-2Rgc-null recipients. Blood *115*, 3704–3707. https://doi.org/10.1182/blood-2009-10-249326.
36. Volk, V., Schneider, A., Spineli, L.M., Grosshennig, A., and Stripecke, R. (2016). The gender gap: discrepant human T-cell reconstitution after cord blood stem cell transplantation in humanized female and male mice. Bone Marrow Transplant. *51*, 596–597. https://doi.org/10.1038/bmt.2015.290.
37. Atreya, R., Mudter, J., Finotto, S., Müllberg, J., Jostock, T., Wirtz, S., Schütz, M., Bartsch, B., Holtmann, M., Becker, C., et al. (2000). Blockade of interleukin 6 trans signaling suppresses T-cell resistance against apoptosis in chronic intestinal inflammation: evidence in crohn disease and experimental colitis in vivo. Nat. Med. *6*, 583–588. https://doi.org/10.1038/75068.
38. Takeda, K., Kaisho, T., Yoshida, N., Takeda, J., Kishimoto, T., and Akira, S. (1998). Stat3 activation is responsible for IL-6-dependent T cell proliferation through preventing apoptosis: generation and characterization of T cell-specific Stat3-deficient mice. J. Immunol. *161*, 4652–4660.
39. Ayroldi, E., Zollo, O., Cannarile, L., D' Adamio, F., Grohmann, U., Delfino, D.V., and Riccardi, C. (1998). Interleukin-6 (IL-6) prevents activation-induced cell death: IL-2-independent inhibition of Fas/fasL expression and cell death. Blood *92*, 4212–4219.
40. Rochman, I., Paul, W.E., and Ben-Sasson, S.Z. (2005). IL-6 increases primed cell expansion and survival. J. Immunol. *174*, 4761–4767. https://doi.org/10.4049/jimmunol.174.8.4761.
41. Yu, C.I., Marches, F., Wu, T.C., Martinek, J., and Palucka, K. (2020). Techniques for the generation of humanized mouse models for immuno-oncology. Methods Enzymol. *636*, 351–368. https://doi.org/10.1016/bs.mie.2019.06.003.

STAR★METHODS

KEY RESOURCES TABLE

REAGENT or RESOURCE	SOURCE	IDENTIFIER
Antibodies		
Human CCR7-PE/Cy7 (3D12)	BD	557648; RRID:AB_396765
Human CD117-BV605 (104D2)	Biolegend	313218; RRID:AB_2562025
Human CD11b-BV711 (D12)	BD	742641; RRID:AB_2740934
Human CD11c-V450 (B-ly6)	BD	560369; RRID:AB_1645557
Human CD138-PE (MI15)	Biolegend	356504; RRID:AB_2561877
Human CD14-AF488 (HCD14)	Biolegend	325610: RRID:AB_830683
Human CD14-PE/Cy7 (MqP9)	BD	562698; RRID:AB_2737729
Human CD141-APC (AD5-14H12)	Miltenyi Biotec	130-090-907; RRID:AB_2733313
Human CD15-FITC (HI98)	Biolegend	301904; RRID:AB_314196
Human CD16-BUV395 (3G8)	BD	563785; RRID:AB_2744293
Human CD185-AF647 (RF8B2)	BD	558113; RRID:AB_2737606
Human CD19-APC (HIB19)	Biolegend	302212; RRID:AB_314242
Human CD19-PE-CF594 (HIB19)	BD	562294; RRID:AB_11154408
Human CD1c-PerCP-Cy5.5 (L161)	Biolegend	331514; RRID:AB_1227536
Human CD20-AF700 (2H7)	Biolegend	302322; RRID:AB_493753
Human CD27-BV711 (M-T271)	Biolegend	356430; RRID:AB_2650751
Human CD279-BV421 (EH12.2H7)	Biolegend	329919; RRID:AB_10900818
Human CD3 (OKT3)	Biolegend	317325; RRID:AB_2749889
Human CD3-APC-H7 (SK7)	BD	560176; RRID:AB_1645475
Human CD3-BV786 (SK7)	BD	563800; RRID:AB_2744384
Human CD3-PE-CF594 (UCHT1)	BD	562280; RRID: AB_11153674
Human CD303-BV785 (201A)	Biolegend	354222; RRID:AB_2572147
Human CD33-PE (P67.6)	Biolegend	366608; RRID:AB_2566106
Human CD38-FITC (HB-7)	Biolegend	356609; RRID:AB_2561949
Human CD4-BUV395 (SK3)	BD	563550; RRID:AB_2738273
Human CD45-BV510 (HI30)	BD	563204; RRID:AB_2738067
Human CD45RA-PerCP/Cy5.5 (HI100)	BD	563429; RRID:AB_2738199
Human CD56-BV605 (NCAM16.2)	BD	562780; RRID:AB_2728700
Human CD66b-AF700 (G10F5)	Biolegend	305114; RRID:AB_2566037
Human CD8-PB (RPA-T8)	BD	558207; RRID:AB_397058
Human HLA-DR APC-H7 (G46-6)	BD	561358; RRID:AB_10611876
Mouse CD103-PerCP/Cy5.5 (M290)	BD	563637; RRID:AB_2738337
Mouse CD11b-APC/Cy7 (M1/70)	TONBO	25-0112-U100; RRID:AB_3094465
Mouse CD11c-V450 (HL3)	BD	560521; RRID:AB_1727423
Mouse CD16/CD32 (2.4G2)	BD	553142; RRID:AB_394657
Mouse CD19-PE-CF594 (1D3)	BD	562291; RRID:AB_11154223
Mouse CD317-APC (927)	Biolegend	127016; RRID:AB_1967101
Mouse CD3e-PE-CF594 (145-2C11)	BD	562286; RRID:AB_11153307
Mouse CD45-BV650 (30-F11)	BD	563410; RRID:AB_2738189
Mouse CD8a-PE (53-6.7)	BD	553032; RRID:AB_394570
Mouse F4/80-PE/Cy7 (BM8)	Biolegend	123114; RRID:AB_893478

(*Continued on next page*)

Continued

REAGENT or RESOURCE	SOURCE	IDENTIFIER
Mouse Ly-6G/Ly-6C-Pacific Orange (RB6-8C5)	ThermoFisher	RM3030; RRID:AB_2556571
Mouse MHC class II-FITC (10-3.6)	BD	553540; RRID:AB_394909
Biological samples		
Human bone marrow	Lonza	1M-125
Human cord blood $CD34^+$ cells	Lonza	2C-101
Chemicals, peptides, and recombinant proteins		
Trypan blue solution	Corning	25-900-CI
7-AAD viability staining solution	Biolegend	420403
BD FACS Lysing solution 10X concentrate	BD	349202
Brilliant stain buffer	BD	563794
Dnase I	Millipore Sigma	D4513-1VL
Fetal bovine Serum	GeminiBio	100-500-500
Heparin (1000 USP units/mL)	Meitheal Pharmaceuticals	NDC71288-402-10
Liberase	Millipore Sigma	5401127001
Lipopolysaccharide	Invivogen	vac-3pelps
MEM non-essential amino acids solution	ThermoFisher	11140050
PBS	ThermoFisher	10010023
Penicillin-streptomycin	ThermoFisher	15070063
PrimSTAR GXL DNA polymerase	TaKaRa Bio USA	R050A
RBC lysis buffer	Biolegend	420301
RPMI 1640 medium	ThermoFisher	21870092
Sodium pyruvate	ThermoFisher	11360070
Critical commercial assays		
Human IL-6 ELISA MAX Deluxe kit	Biolegend	430504
Mouse Flt-3 Ligand/FLT3L DuoSet ELISA kit	R&D Systems	DY427
NucleoSpin Tissue kit	TaKaRa Bio USA	740952
NucleoSpin® Gel and PCR Clean-Up kit	TaKaRa Bio USA	740609
Experimental models: Organisms/strains		
Mouse: NSG	The Jackson Laboratory	RRID: IMSR JAX:005557
Mouse: NSGF	This paper; The Jackson Laboratory	RRID: IMSR_JAX:035842
Mouse: NSGF6	This paper	N/A
Oligonucleotides		
Primers for *Flt3* KO, see Table S1	This paper	N/A
Primers for *IL6* KI, see Table S1	This paper	N/A
Primers for donor DNA backbone, see Table S1	This paper	N/A
Murine *Flt3* exon 3 sgRNA: AAGTGCAGCTCGCCACCCCA	This paper	N/A
Murine *Il6* exon 1 sgRNA: TGCAGAGAGGAACTTCATAG	This paper	N/A
Murine *Il6* exon 1 sgRNA: AGGAACTTCATAGCGGTTTC	This paper	N/A
Murine *Il6* exon 5 sgRNA: ATGCTTAGGCATAACGCACT	This paper	N/A
Recombinant DNA		
Recombinant human *IL6* DNA	Genescript	IL6-201
Software and algorithms		
Flowjo 10.9.0	BD	RRID:SCR_008520
Prism 9 & 10	GraphPad Software	RRID:SCR_002798
Benchiling	Biology Software	RRID:SCR_013955

RESOURCE AVAILABILITY

Lead contact

Further information and requests for resources and reagents should be directed to and will be fulfilled by the lead contact, Karolina Palucka (karolina.palucka@jax.org).

Materials availability

Murine mouse models generated in this study, namely NSGF and NSGF6 mice, are available from the lead contact's laboratory upon request.

Data and code availability

All data reported in this paper will be shared by the lead contact upon request. This paper does not report original code. Any additional information required to reanalyze the data reported in this paper is available from the lead contact upon request.

EXPERIMENTAL MODEL AND STUDY PARTICIPANT DETAILS

Genetic engineering of mouse models

All mice were obtained from The Jackson Laboratory (Bar Harbor, ME). The protocol on genetic engineering of mouse models was reviewed and approved by the Institutional Animal Care and Use Committee at The Jackson Laboratory (14005). Mouse *Flt3* KO mice (NOD.Cg-Prkdc^{scid} *Il2rg*^{tm1Wjl}-*Flt3*^{em1Akp}; NSGF; RRID:IMSR JAX:035842) were generated by CRISPR using Cas9 mRNA and single-guide RNA (sgRNAs) (5′-AAGTGCAGCTCGCCACCCCA-3′) targeting exon 3 of mouse *Flt3* in fertilized eggs of NSG mice (NOD.Cg-Prkdc^{scid} *Il2rg*^{tm1Wjl}/SzJ; RRID:IMSR JAX:005557) following previous published protocol.[34] The blastocysts derived from the injected embryos were transplanted into foster mothers and newborn pups were obtained. Founders and F1 littermates were tail tipping and tested for successful gene-knockout by PCR and Sanger sequencing. Mice carrying a null deletion were backcrossed to NSG for two generations and were then interbred until all offspring were homozygous for *Flt3* KO mutation. Human *IL6* KI mice (NOD.Cg-*Prkdc*^{scid} *Il2rg*^{tm1Wjl}-*Flt3*^{em1Akp}*Il6*$^{emX(IL6)Akp}$; NSGF6) were generated using CRISPR/cas9 system. sgRNAs were designed to target exon 1 (5′-TGCAGAGAGGAACTTCATAG-3′ or 5′-AGGAACTTCA TAGCGGTTTC-3′) *and* exon 5 (5′-ATGCTTAGGCATAACGCACT-3′) of mouse *Il6* locus. Cas9 mRNA, sgRNAs targeting mouse *Il6* locus and recombinant human *IL6* DNA were coinjected into fertilized NSGF oocytes. Human *IL6* was inserted into exon 1 and exon 5 via homologous recombination. The resulting founders, carrying human *IL6* were bred to NSGF mice for two generations, and were then interbred until all offspring were homozygous for *Il6* targeted mutation. For human IL-6 production, mice at 6–8 weeks of age were treated once with 0.1–10 μg of LPS (InvivoGen, San Diego, CA) i.p. and euthanized after 2 h for plasma collection.

Humanized mice

Humanized mice were generated on mice obtained from The Jackson Laboratory (Bar Harbor, ME). All protocols were reviewed and approved by the Institutional Animal Care and Use Committee at The Jackson Laboratory (14005) and University of Connecticut Health Center (101163-0220 and 102195-1122; Farmington, CT). Female mice were sub-lethally irradiated (10 cGy per gram of body weight) using gamma irradiation at four weeks of age. Human CD34$^+$ HSPCs isolated from full-term cord blood (Lonza) or adult bone marrow (Lonza) were given by tail-vein intravenous (i.v.) injection in 200 μL of PBS with 1 μg/mL of anti-CD3 antibody (OKT3, Biolegend). The donors of human CD34$^+$ HSPCs were obtained from commercial sources which have been tested negative for blood-borne pathogens (HIV, HBV, and HCV) by vendors but have not been tested for CMV or EBV. The donors were randomly selected without the knowledge of any demographic information (age or gender). Monthly post HSPC transplant, one capillary tube of blood (60–70 μL) was collected using heparin-coated hematocrit tubes (Drummond Scientific) and mixed with 5 USP units of heparin (5 μL) by retro-orbital bleeding from the mice to evaluate blood engraftment.[41] To determine the absolute white blood cell count, red blood cells (RBC) was first lysed by mixing 5 μL of heparin blood with 20 μL of BD FACS Lysing solution for 5 min. Total cell count was performed on RBC-lysed blood using Neubauer hemocytometer (Hausser Scientific) with 0.4% Trypan blue (Corning). The absolute white blood cell count was then enumerated after accounting for the dilution factor from each step. The remaining blood was used for immunophenotyping by flow cytometry. Mice were euthanized according to the individual experimental design.

METHOD DETAILS

Genotyping assays

For all founders, the mice were typed by PCR reaction for the presence or absence of the *Flt3* KO and human *IL6* KI sequence using primers listed in Table S1. Genomic DNA was isolated from tail biopsies using the NucleoSpin Tissue kit (TaKaRa Bio USA, San Jose, CA) following manufacture protocols. All primers were purchased from Eurofins Genomics (Louisville, KY). PCR reactions were performed with PrimSTAR GXL DNA polymerase (TaKaRa Bio USA) with 1 μL of genomic DNA and 0.2 μM primers. A common PCR thermal-cycle amplification program was used for all primer pairs (10 s at 98°C and 1–3 min at 68°C for 30 cycles). PCR products were run on agarose gels and size was estimated with comparison to a DNA mass ladder. In some experiment, the remaining PCR products were extracted with PCR cleanup kit (TaKaRa Bio USA) and sequenced to confirm the correct gene sequence.

Tissue processing for flow cytometry

For immunophenotype, tissues including blood, bone marrow, spleen and lungs were collected. Bone marrow was harvested from femur and tibia by flushing out the marrow. Spleen was digested with 50 μg/mL of Liberase (Millipore Sigma) and DNase I (Millipore Sigma) for 10 min at 37°C. Lungs were digested with 50 μg/mL of Liberase and DNase I for 30 min at 37°C, followed by mechanical dissociation with GentleMACS (Miltenyi Biotec, Bergisch Gladbach, Germany). Single cell suspensions were made, and the debris was removed by filtering through 70 μm cell strainers. Cells were first treated with RBC lysis buffer (Biolegend) to remove red blood cells. Total cell counts were measured in hemocytometer with 0.4% trypan blue. Single cell suspensions were treated with Fc blocker (BD), and then stained on ice with antibody cocktail for 30 min. After washing twice with PBS, samples were resuspended in buffer (PBS, 2% FBS, 2 mM EDTA), acquired on a Symphony A5 (BD) and analyzed with FlowJo software (BD). The absolute cell count for each cell type was determined by multiplying total cell counts by the differential percentage of each cell type.

For the analysis of mouse DCs, cells were stained with antibodies to mouse CD45-BV650 (30-F11, BD), CD3-PE-CF579 (145-2C11, BD), $CD19^{-}$ PE-CF579 (ID3, BD), CD103-PerCP-Cy5.5 (M290, BD), F4/80-PE-Cy7 (BM8, Biolegend), Ly-6G/Ly-6C-Pacific Orange (RB6-8C5, ThermoFisher), MHC class II-FITC (10-3.6, BD), CD11c-V450 (HL3, BD), CD8-PE (53-6.72, BD), and CD317-APC (927, Biolegend). For human engraftment in the blood, cells were stained with mCD45-BV650 (30-F11, BD), and antibodies to human CD45-BV510 (HI30, BD), CD14-AF488 (HCD14, Biolegend), CD33-PE (P67.6, Biolegend), CD19-APC (HIB19, Biolegend) and CD3-APC-H7 (SK7, BD). Occasionally cells were stained with additional antibodies including CD45RA-PerCPCy5.5 (HI100, BD), CCR7-PE-Cy7 (3D12, BD), CD8-PB (RPA-T8, BD) and CD4-BUV395 (SK3, BD) for T cell phenotype. For cellular composition in tissues, cells were stained with antibody cocktail containing mCD45-BV650, hCD45-BV510, CD15-FITC (HI98, Biolegend), CD1c-PerCP-Cy5.5 (L161, Biolegend), CD33-PE, CD3-PE-CF594 (UCHT1, BD), CD19-PE-CF594 (HIB19, BD), CD14-PE-Cy7, CD141-APC (AD5-14H12, Miltenyi Biotec), CD66b-AF700 (G10F5, Biolegend), HLA-DR-APC-H7 (G46-6, BD), CD11c-V450 (B-ly6, BD), CD117-BV605 (104D2, Biolegend), CD11b-BV711 (D12, BD), CD303-BV785 (201A, Biolegend), and CD16-BUV395 (3G8, BD) in Brilliant Stain Buffer Plus (BD) for myeloid phenotype; and antibody cocktail containing antibodies to mCD45-BV650, hCD45-BV510, CD38-FITC (HB-7, Biolegend), CD45RA-PerCP-Cy5.5, CD138-PE (MI15, Biolegend), CD19-PE-CF594, CCR7-PE-Cy7, CD185-AF647 (RF8B2, BD), CD20-AF700 (2H7, Biolegend), CD8-APC-H7 (HIT8a, BD), CD279-BV421 (EH12.2H7, Biolegend), CD56-BV605 (NCAM16.2, BD), CD27-BV711 (M-T271, Biolegend), CD3-BV786 (SK7, BD) and CD4-BUV395 for lymphoid phenotype. Viability dye 7-AAD (Biolegend) were added to samples before acquisition on a flow cytometer.

ELISA

ELSA were performed following manufacture protocols. For mouse Flt3L, plasma was tested with mouse Flt3L ELISA Duo Set from R&D systems. For human IL-6, plasma was tested with human IL-6 ELISA MAX Deluxe Set from Biolegend.

QUANTIFICATION AND STATISTICAL ANALYSIS

Statistical analyses were performed in Prism (GraphPad, San Diego, CA). Data were graphed as the mean ± standard deviation (SD). Legend is: ****$p < 0.0001$, ***$p < 0.001$, **$p < 0.01$, *$p < 0.05$, ns = not significant. Comparisons between any 2 groups were analyzed using the Mann-Whitney test or two-tailed t-test. Comparisons between any 3 or more groups were analyzed by analysis of variance (ANOVA).